Please cite this article in press as: Fernando et al., Polysaccharide assemblies in fungal and plant cell walls explored by solid-state NMR, Structure (2023), https://doi.org/10.1016/j.str.2023.07.012

Structure

CellPress

Review

Polysaccharide assemblies in fungal and plant cell walls explored by solid-state NMR

Liyanage D. Fernando,[1,2] Wancheng Zhao,[1,2] Isha Gautam,[1] Ankur Ankur,[1] and Tuo Wang[1,*]
[1]Department of Chemistry, Michigan State University, East Lansing, MI 48824, USA
[2]These authors contributed equally
*Correspondence: wangtuo1@msu.edu
https://doi.org/10.1016/j.str.2023.07.012

SUMMARY

Structural analysis of macromolecular complexes within their natural cellular environment presents a significant challenge. Recent applications of solid-state NMR (ssNMR) techniques on living fungal cells and intact plant tissues have greatly enhanced our understanding of the structure of extracellular matrices. Here, we selectively highlight the most recent progress in this field. Specifically, we discuss how ssNMR can provide detailed insights into the chemical composition and conformational structure of pectin, and the consequential impact on polysaccharide interactions and cell wall organization. We elaborate on the use of ssNMR data to uncover the arrangement of the lignin-polysaccharide interface and the macrofibrillar structure in native plant stems or during degradation processes. We also comprehend the dynamic structure of fungal cell walls under various morphotypes and stress conditions. Finally, we assess how the combination of NMR with other techniques can enhance our capacity to address unresolved structural questions concerning these complex macromolecular assemblies.

INTRODUCTION

The cell walls of plants and fungi play vital roles in cell shape, mechanics, integrity, adhesion, and extensibility.[1–4] These macromolecular assemblies are also crucial for energy and carbon storage, as well as antimicrobial resistance, and serve as potential targets for novel antifungal agents.[5,6] From a structural perspective, cell walls represent highly sophisticated biomaterials created by nature, inspiring extensive efforts to develop artificial materials that mimic the chemical and physical principles governing macromolecular assembly.[7,8] However, the characterization of such nanocomposites in their native state presents significant challenges.

Recent advancements in solid-state NMR (ssNMR) techniques have enabled high-resolution investigation of cell wall materials by leveraging methods initially developed for NMR structural biology of proteins, nucleic acids, and polymers.[9–12] This approach has been adopted due to the sufficient spectroscopic resolution available, which allows for the acquisition of numerous structural constraints to visualize the complex composition of biomolecules within cell walls. Additionally, it addresses the limitations posed by the inherent heterogeneity and complexity of the cell wall by utilizing simplified representations.[13] Extensive studies have been conducted on numerous plant and fungal species, leading to significant revisions in our understanding of cell wall structure.[14] In this review, we aim to provide a concise overview of the key principles in ssNMR methodology and the most recent structural findings, with a focus on those published within the past three years.

METHODOLOGY ADVANCES ENABLING ssNMR OF CELLULAR SAMPLES

One of the major merits of ssNMR lies in its ability to directly characterize living cells or intact tissues.[15,16] Since solubilization or extraction is not necessary, the samples fully preserve the inherent physical and chemical characteristics of the biomolecules. The samples analyzed are typically enriched with NMR-active isotopes by incorporating ^{13}C-enriched precursors like ^{13}C-glucose, ^{13}C-maltose, and $^{13}CO_2$ (for plants), as well as ^{15}N-labeled amino acids and salts.[17,18] Occasionally, selective-labeled precursors are used to simplify the spectra and track the biosynthesis of macromolecules.[19] Deuterated fatty acids can also be incorporated for determining the phospholipid profile in cellular membranes.[20] The collected material can be directly placed into a magic-angle spinning (MAS) rotor, which can hold approximately between 1 mg (for a 0.7 mm diameter) and 100 mg (for a 4 mm diameter) of material, depending on the requirements of the NMR experiment.

A versatile toolbox is available for studying various aspects of biomolecules in cell walls and cellular samples, including molecular composition, structural variations, dynamical distribution, water association, and sub-nanometer packing.[13,14,21] While 1D spectra are useful for quick screening, high-resolution structural characterization often mandates the use of 2D and 3D homonuclear (such as ^{13}C–^{13}C) and heteronuclear (such as ^{15}N/^{1}H-^{13}C) correlation experiments. These techniques rely primarily on ^{13}C detection, which provides excellent spectral dispersion to differentiate many magnetically inequivalent sites.[22–27] However, recent advancements in ^{1}H detection

Please cite this article in press as: Fernando et al., Polysaccharide assemblies in fungal and plant cell walls explored by solid-state NMR, Structure (2023), https://doi.org/10.1016/j.str.2023.07.012

methods have also yielded valuable insights into the structure and packing of polysaccharides and proteins in plants, fungi, and bacteria.[28–31] The success of these studies has been facilitated by fast-to-ultrafast magic-angle spinning techniques, with MAS rotation frequencies ranging from 60 to 110 kHz, where a higher level of deuteration and the presence of more dynamic molecules allow for reduced reliance on high MAS frequencies.

Dynamic nuclear polarization (DNP) is another significant advancement that has greatly expanded the capabilities of ssNMR in the structural characterization of macromolecular complexes.[32–34] In MAS-DNP, the polarization of unpaired electrons in stable biradicals is transferred to ^{1}H and subsequently to other nuclei of interest, resulting in enhanced sensitivity.[35] The prominent biradicals used extensively in structural studies include AMUPol and the recently developed AsympolPOK.[36,37] The 600 MHz/395 GHz MAS-DNP instrument strikes a favorable balance between spectral resolution and sensitivity enhancement, and a 30- to 80-fold boost can be easily achieved for cellular samples. This breakthrough has effectively overcome the sensitivity limitations of NMR, enabling the use of small sample quantities, which is particularly valuable for difficult-to-replicate samples, exploring lowly populated molecules or macromolecular complexes embedded in bulk structures, and even characterizing fully unlabeled biosamples without the need for isotopic enrichment.[38–43]

PECTIN METHYLATION INFLUENCING PLANT PRIMARY CELL WALL STRUCTURE

The mechanical roles of cellulose microfibrils, hemicellulose, and pectin in plant primary cell walls have been a topic of ongoing debate for many decades.[44] One prevailing model suggests the existence of a tethered polymer network, where a single hemicellulose strand (e.g., a xyloglucan) could simultaneously bind to multiple cellulose microfibrils and hold them together to form a load-bearing network.[45,46] Pectin is an acidic polymer regulating wall porosity, pH, and ionic balance, and is influencing cell expansion and differentiation.[47] However, pectin is often considered as a separate component that forms a gel-like matrix, providing reinforcement to the cellulose-hemicellulose network. This perspective was primarily based on biochemical findings, wherein the vast majority of pectin is extractable by strong alkali, and the acidic pectin backbones do not bind to cellulose *in vitro*.[48] A significant advancement brought in by ssNMR is the identification of the interaction between pectin and cellulose within intact primary plant cell walls.

Pectins are partially interconnected complexes of polysaccharides and proteoglycans.[47,49,50] The major domains include homogalacturonan (HG), rhamnogalacturonan-I (RG-I) with branched arabinan and galactan, as well as RG-II.[51] By employing ssNMR, even with a simple 1D ^{13}C spectrum, it is possible to discern various specific chemical sites within the galacturonic acid (GalA) residues that comprise HG, the rhamnose (Rha) residues that alternate with GalA along the RG-I backbone, as well as the arabinan sidechains (Figure 1A).[52] Such spectral resolution forms the basis for tracking the intermolecular cross peaks between major pectin domains and cellulose microfibrils using 2D ^{13}C–^{13}C correlation experiments.[53,54] However, RG-II, which is less prevalent and structurally more intricate compared to HG and RG-I, has yet to be investigated using high-resolution ssNMR techniques.

Previously, it was believed that the pectin backbone and cellulose were physically separated entities, but the numerous pectin-cellulose cross peaks identified by ssNMR have unambiguously revealed their close spatial proximity in the cell wall.[54,55] The new insight has contributed to a paradigm shift in our understanding of the architecture of the primary cell wall,[44,56] and comprehensive overviews of these ssNMR studies can be found in multiple recent reviews.[14,57] Despite these advancements, the precise function of the packing between pectin and cellulose in supporting the structure of the cell wall remains unclear. Recently, mesoscale coarse-grained molecular dynamics (CGMD) simulations conducted on onion epidermal cell walls have shed some light on this matter.[58] The noncovalent interactions between multiple cellulose fibrils were found to be the primary factor determining the mechanical properties of the cell wall. Notably, the sliding of two aligned cellulose microfibrils against each other was identified as a significant contributor to the plasticity of the cell wall. In contrast, hemicellulose and pectin were suggested to play more indirect roles, potentially by influencing the arrangement of cellulose within the cell wall.[58]

Growing evidence emphasizes the significance of HG methylation in influencing the organization of the cell wall. At first glance, this may appear contradictory, as methylation only involves localized chemical modifications to the carboxyl groups of GalA residues,[59,60] while the rearrangement of cell wall polymers happens on the nanoscale. An emerging concept is that methylation alters the charge and physicochemical properties of HG, and may induce repulsion among HG chains, thereby providing the force to expand the interfibrillar space between cellulose microfibrils.[61] This mechanism has been proposed as a potential regulator of cell expansion and shaping, alongside the more widely accepted turgor-driven mechanism.

Dupree, Hong, and coworkers have shown that pectin methylation can change the conformational structure, interactions, and dynamics of polysaccharides in the primary cell wall.[62] They compared the pectin structure in wild-type *Arabidopsis* with that of the *gosamt1 gosamt2* mutant, which had a reduced degree of methyl esterification in HG. The mutant exhibited an increased abundance of HG in a structure known as the 2-fold screw conformation (2_1), with its C6 chemical structure as -COO^- in this sample (Figure 1B). These observations match the characteristics of the egg-box structure that refers to the cross-linking of two anionic GalA units that joined two adjacent HG chains by a Ca^{2+} ion. The reduced methyl esterification in the mutant promoted the formation of egg-box clusters and enhanced HG aggregation.

Conversely, the content of the methylated -$COOCH_3$ motif in the 3-fold screw conformation (3_1) was reduced in the *gosamt1 gosamt2* mutant.[62] The double mutant also exhibited strong signals indicating a reduction in the chain length of HG, allowing the identification of signals from the reducing ends of the GalA units in both α- and β-configurations. Importantly, this study represents the first successful application of ssNMR to elucidate the detailed structural characteristics of HG *in muro*, providing direct experimental evidence supporting the widely accepted model of the pectin egg-box structure within the plant cell wall.

Please cite this article in press as: Fernando et al., Polysaccharide assemblies in fungal and plant cell walls explored by solid-state NMR, Structure (2023), https://doi.org/10.1016/j.str.2023.07.012

CellPress

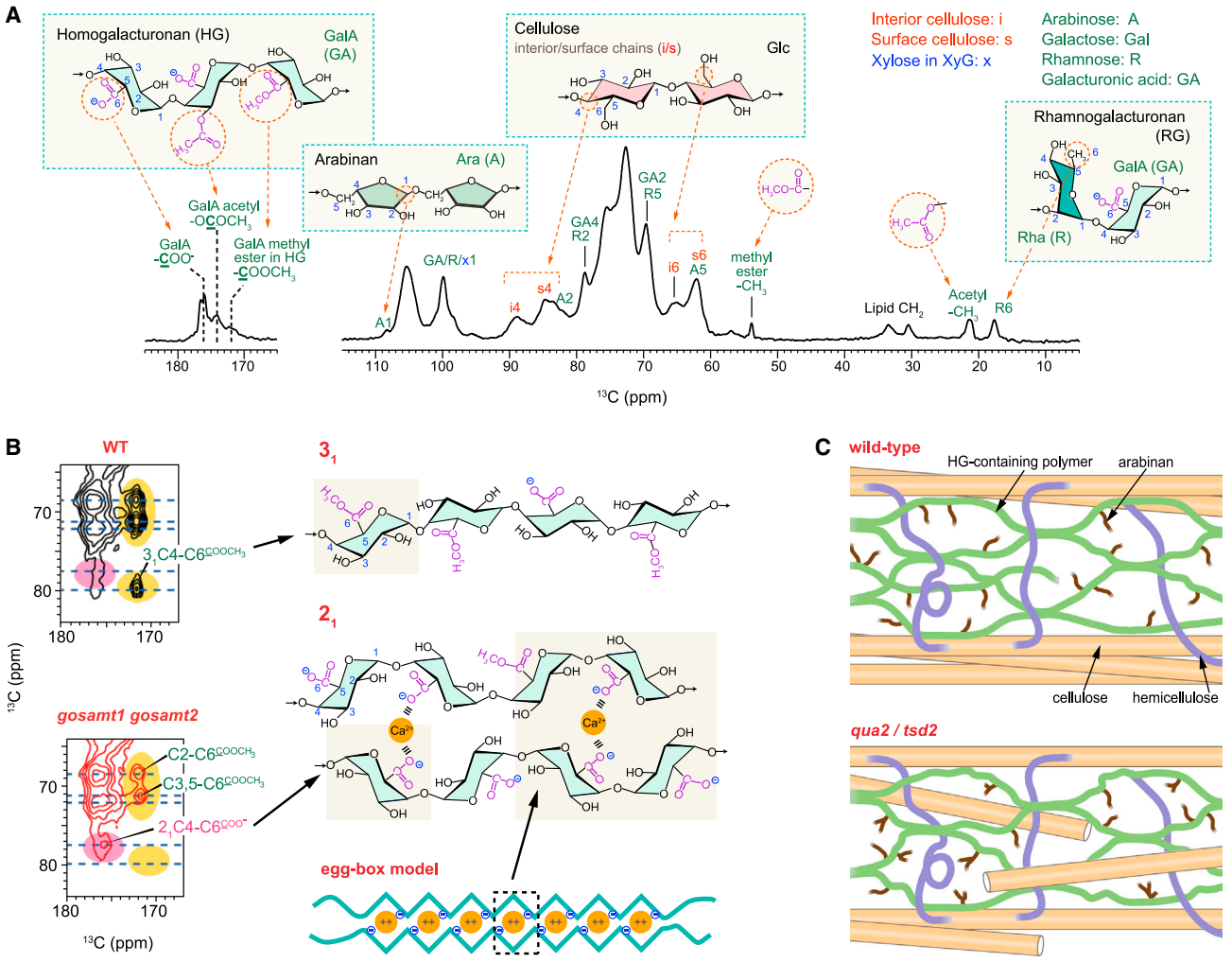

Figure 1. Pectin structure and its effect on primary plant cell wall

(A) Representative 1D ^{13}C ssNMR spectra with resolvable signals associated with pectin and cellulose structural motifs. Carbon numbers are shown for key sugar units.

(B) Selected regions of 2D ^{13}C–^{13}C spectra resolving the conformation and methylation state of GalA units in *Arabidopsis* pectin. 2-fold (2_1) and 3-fold (3_1) screw conformations of HG displaying distinct chemical environments at the carbonyl site. An egg-box model is shown to depict two cross-linked HG chains.

(C) Structural rearrangement of the cell wall in *Arabidopsis* qua2/tsd2 mutant. Figures 1A and 1C adapted with permission from Kirui et al. *Carbohydr. Polym.* (2021). Figure 1B adapted with permission from Temple et al. *Nat. Plants* (2022).

NMR data showed that HG methylation has an impact on the polysaccharide organization in the cell wall. Pectin backbones showed larger dipolar order parameters and stronger interactions with cellulose in the *gosamt1 gosamt2* mutant.[62] These changes in cell wall structure were found to be associated with impaired polarized growth in the double mutant. Interestingly, these findings appear to contrast with recent observations from other studies using different mutants and experimental conditions. An increase in pectin methylation is often accompanied by stronger pectin-cellulose interactions and impaired plant growth as reported in ssNMR analyses of *Arabidopsis* primary cell walls and focused on mutants that produced shorter HG chains, cell walls with pH-alteration, or segments along the inflorescence stem.[63–65]

The situation becomes more intricate due to another recent study involving two allelic mutants (*qua2* and *tsd2*) of a pectin methyltransferase.[52] These mutants exhibit similar cell wall composition and pectin methyl esterification levels as the wild-type sample but, surprisingly, display stiffer pectin and stronger interactions with cellulose (Figure 1C). Atomic force microscopy (AFM) and field emission scanning electron microscopy (FESEM) revealed a decrease in cellulose bundling in both mutants,[66] and the more dispersed microfibril arrangement should have facilitated the extensive interactions as observed by ssNMR analysis.

These findings highlight how ssNMR can serve as a valuable tool to bridge the knowledge gaps between the chemical structure of carbohydrates, plant biology, and cell wall organization. However, pectin's role in cell wall structure remains enigmatic. It is now evident that pectin methylation can exert diverse effects on the cell wall structure, and there is no universal principle that applies to all scenarios. It is likely that the structural function of pectin is indirect, influencing the arrangement of cellulose

Please cite this article in press as: Fernando et al., Polysaccharide assemblies in fungal and plant cell walls explored by solid-state NMR, Structure (2023), https://doi.org/10.1016/j.str.2023.07.012

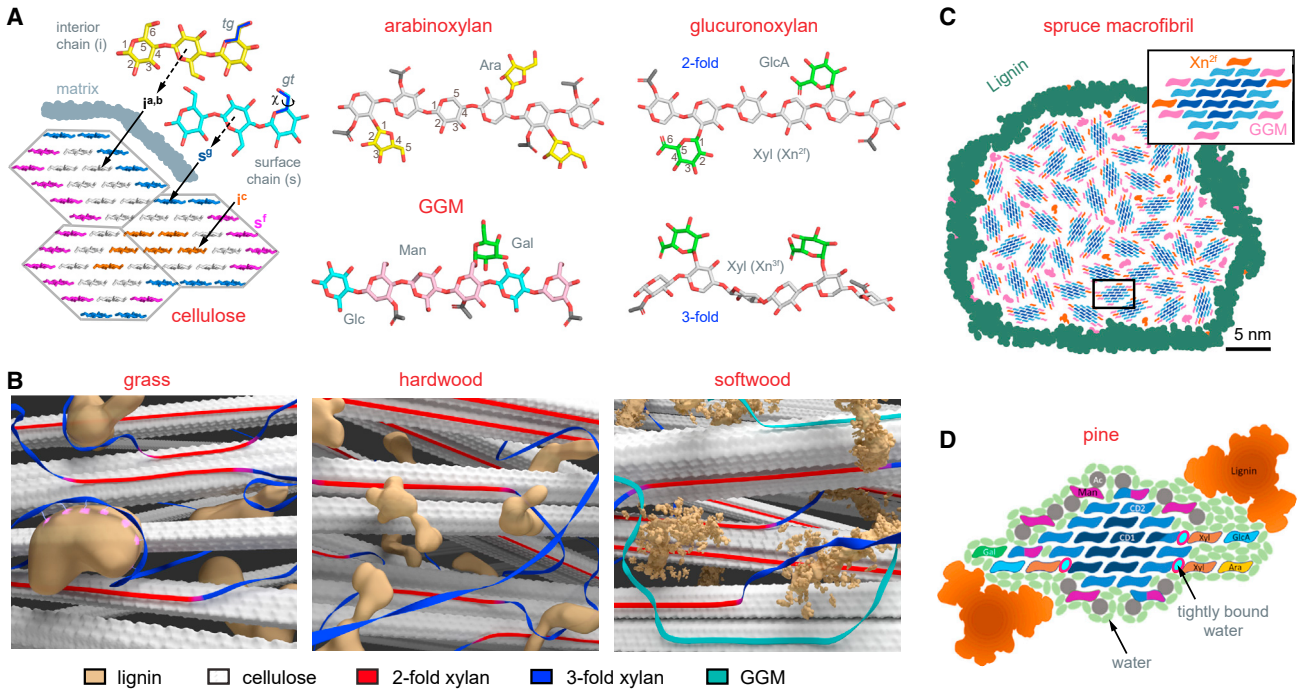

Figure 2. Macrofibril structure and lignin-carbohydrate interface

(A) Structural features of polysaccharides in plant secondary cell walls resolvable by ssNMR.

(B) Structural view of the aromatic-carbohydrate packing interface in grass species, hardwood, and softwood.

(C) Best fit of NMR data collected on spruce secondary cell walls into a macrofibril. A local cellulose microfibril with two domains of glucan chains (light and dark blue) is shown with 2-fold xylan (Xn^{2f}) and galactoglucomannan (GGM) attached.

(D) Illustration of loosely associated water and tightly bound water in pine secondary cell wall. Figures 2A and 2B adapted from Kirui et al. *Nat. Commun.* (2022). Figure 2C modified from Terrett et al. *Nat. Commun.* (2019). Figure 2D adapted from Cresswell et al. *Biomacromolecules* (2021).

microfibrils and hemicellulose within the cell wall, which requires further investigation.

LIGNIN-CARBOHYDRATE PACKING IN SECONDARY PLANT CELL WALLS

Within the secondary cell wall, the coalescence of multiple cellulose microfibrils occurs frequently, e.g., an illustration of a 3-microfibril bundle is given in Figure 2A, which is accompanied by the association of hemicelluloses (xylan and galactoglucomannan) and lignin to form larger macrofibrils.[67,68] Inspired by the seminal work of Dupree and colleagues,[69] many multidimensional ssNMR studies have been conducted in the past seven years to unravel the molecular architecture of secondary plant cell walls. These studies have led to two significant revisions in our understanding of lignocellulosic biomass. First, the chemical composition and conformational structure of xylan dictate its binding specificity within the cell wall.[70,71] Second, the lignin-carbohydrate interface is stabilized by electrostatic interactions, with lignin primarily associated with the non-flat domains of xylan. However, in certain cases, lignin can also interact and co-localize with the xylan-coated cellulose microfibrils as the secondary target.[72,73]

In dehydrated environments, such as the dried stem of *Arabidopsis*, xylan exhibits a broad range of helical screw conformations that can be monitored through the continuous band observed in its C4 signals in ssNMR spectra.[69] In well-hydrated cell walls, including those of *Arabidopsis*, spruce, maize, switchgrass, rice, and *Brachypodium*, xylan preferentially adopts either 2-fold or 3-fold helical screw conformations, resulting in two distinct C4 signals.[70,72–74] This is illustrated by the flat-ribbon and non-flat structures depicted in Figure 2A. Notably, a continuous distribution of xylan helical screw conformation was even observed in hydrated hardwood materials, such as eucalyptus and poplar, which is likely induced by factors such as lower hydration levels and/or molecular crowding within hardwood stems.[73] In the case of sorghum, the secondary cell wall is primarily composed of 3-fold xylan conformations,[75] while in *Brachypodium*, both the leaf and root showed two xylan conformers, but the stem shows a continuous range of conformations.

The presence of a 2-fold flat-ribbon structure is relatively uncommon and was found to be facilitated by xylan's deposition onto the smooth surface of a cellulose microfibril.[76] Moreover, it has been discovered that an evenly distributed pattern of substitutions (e.g., by glucuronic acid or arabinose sidechains) along the xylan chain is crucial for maintaining this flat-ribbon structure and promoting its interaction with cellulose.[71] This also explains why sorghum lacks this conformation as xylan is frequently and irregularly substituted by arabinosyl residues. On the other hand, the 3-fold xylan plays a dominant role in carbohydrates' interactions with lignin, primarily through the polar functional groups, which highlights the significance of electrostatic interactions in stabilizing the interface between lignin nanodomains and carbohydrates (see the grass model in Figure 2B).[72]

Please cite this article in press as: Fernando et al., Polysaccharide assemblies in fungal and plant cell walls explored by solid-state NMR, Structure (2023), https://doi.org/10.1016/j.str.2023.07.012

The molecular architecture of lignin-carbohydrate interactions varies across different plant species (Figure 2B). Comparisons between grasses, hardwoods, and softwoods have revealed a gradual decrease in the domain size and polymer separation between lignin and polysaccharides. Lignin-cellulose packing interactions, which were found to be relatively limited in grass samples, also became abundant in woody plants.[73] During the analysis of the sparsely populated biopolymer interface, which exhibits structural deviations from the overall equilibrium state of the entire cell wall, ssNMR experiments employing spectral editing (e.g., the selected polarization of lignin aromatics or methoxy group or xylan acetyls) selection and DNP enhancement have proven to be instrumental.[77,78]

Dupree and coworkers successfully fit the ssNMR data on molecular fraction, polymer conformation, and polymer spatial proximity into a macrofibril observed under Cryo-SEM (Figure 2C).[74] This large bundle that is tens of nanometers across accommodates ~50 elementary microfibrils, each of which consists of 18 glucan chains. SsNMR analysis uncovered two distinct conformations for galactoglucomannan (GGM), reminiscent of the functional conformations in xylan. It was found that GGM undergoes conformational changes when bound to cellulose in a semi-crystalline manner. Some of the bound GGMs and 2-fold xylan molecules can attach to the surface of the same microfibril, while the other GGMs contribute to the matrix alongside 3-fold xylan. The entire carbohydrate core is enveloped by a lignin layer, completing the molecular architecture of the microfibril assembly.

Water is another important structural component of the secondary cell wall, and high-temperature (105°C) oven-drying can induce irreversible alteration to the structure of Monterey pine (Pinus radiata), even after subsequent rehydration.[79] SsNMR analysis of the rehydrated sample revealed a tighter packing between xylan and cellulose, along with the separation of some mannan into the mobile phase, adopting a conformation similar to that observed in solution. These results support the hypothesis that water plays a crucial role in mediating the packing interactions between xylan and cellulose (Figure 2D). Importantly, this study provides direct evidence of the irreversible change in biomass ultrastructure caused by harsh drying procedures. It should be noted that another ssNMR study has demonstrated fully reversible changes of spruce and poplar through the process of lyophilization and rehydration.[73]

Li, Kang, Yelle, and colleagues have utilized ssNMR to investigate the perturbation of lignin linkages and lignin-polysaccharide packing by termite digestion.[80] This was accomplished by feeding ^{13}C-labeled sapwood sections of Canadian poplar (a natural hybrid *Populus* × *canadensis*), a hardwood, to a phylogenetically higher termite species (*Nasutitermes*) and Monterey pine, a softwood, to a lower termite species (*Cryptotermes*). The abundance of different lignin linkages and lignin-polysaccharide interactions in the termite diet and feces was assessed using 2D ^{13}C–^{13}C radio frequency-driven recoupling (RFDR) and long-range proton-driven spin diffusion (PDSD) spectra. Both termite species were found to effectively dissociate the electrostatic interface between lignin and polysaccharides, but only the lower termite species can perturb the structure of the residual lignin. This study highlights the remarkable capability of ssNMR spectroscopy in examining the structural changes occurring in lignocellulosic materials, and the same approach can be applied to investigate biomass degradation by various biological agents such as white/brown-rot fungi, as well as in industrial processes.[81]

DYNAMIC STRUCTURE OF FUNGAL CELL WALL: CHALLENGE AND OPPORTUNITY

Stark and colleagues have been at the forefront of utilizing ssNMR for nearly two decades to study melanin deposition and its interactions with cell wall polysaccharides in *Cryptococcus* and *Saccharomyces* species.[19,82–85] Recent ssNMR investigations on *Aspergillus* and *Schizophyllum*, with a focus on the cell wall structures, were largely inspired by these studies, and were built upon research strategies employed in plant cell wall characterization, albeit with methodological adaptations.[57,86] However, an unexpected problem that significantly impeded progress was the dynamic nature of fungal cell walls, characterized by their remarkable ability to adapt to varying growth conditions and environmental contexts.[2,87] These microorganisms exhibit an impressive capacity to compensate for the absence of specific polysaccharides through complex biosynthetic reactions, thereby generating a structurally intact cell wall.[88] Such adaptability, unlike their plant counterparts, challenges the notion that certain cell wall polysaccharides, such as cellulose and pectin in primary cell walls, are essential. The dynamic structural changes in fungal cell walls not only enable the survival and adaptation of these microbes to diverse environments but also present technical barriers to our fundamental understanding of these organelles and the development of antifungal medications to combat invasive infections.[89] As a result, it is crucial to carefully monitor the status of the samples and ensure the reproducibility of the culture conditions. In many cases, it becomes necessary to prepare fresh batches of samples specifically for lengthy experiments. Complications further arise from the distinct composition and assembly of biomacromolecules in different fungal species and the vast array of mutant strains found in nature. Therefore, it is crucial to first identify the conserved features of fungal cell walls and elucidate the structural functions of their key polysaccharides before investigating the variations across the wide spectrum of fungal species and strains.

MORPHOTYPE-DEPENDENT STRUCTURE OF *ASPERGILLUS* CELL WALLS

During the transition of morphotypes in the fungal life cycle, the cell wall undergoes significant changes in its nanoscale morphology and molecular composition.[2,90] These structural transformations play a vital role in many biological processes, such as spore germination, hyphal growth, and sporulation. In the case of *A. fumigatus*, the fungus forms asexual hydrophobic spores called dormant conidia (dorC) on a specialized hyphal structure called conidiophore.[1] In immunocompromised patients, when the inhaled conidia reach the alveoli in the lungs within 4–6 h, the germination process takes place. Germination involves the uptake of water by the conidia, resulting in their swelling and transformation into swollen conidia (swoC). Subsequently, the swollen conidia germinate (gerC) into short hyphae

Please cite this article in press as: Fernando et al., Polysaccharide assemblies in fungal and plant cell walls explored by solid-state NMR, Structure (2023), https://doi.org/10.1016/j.str.2023.07.012

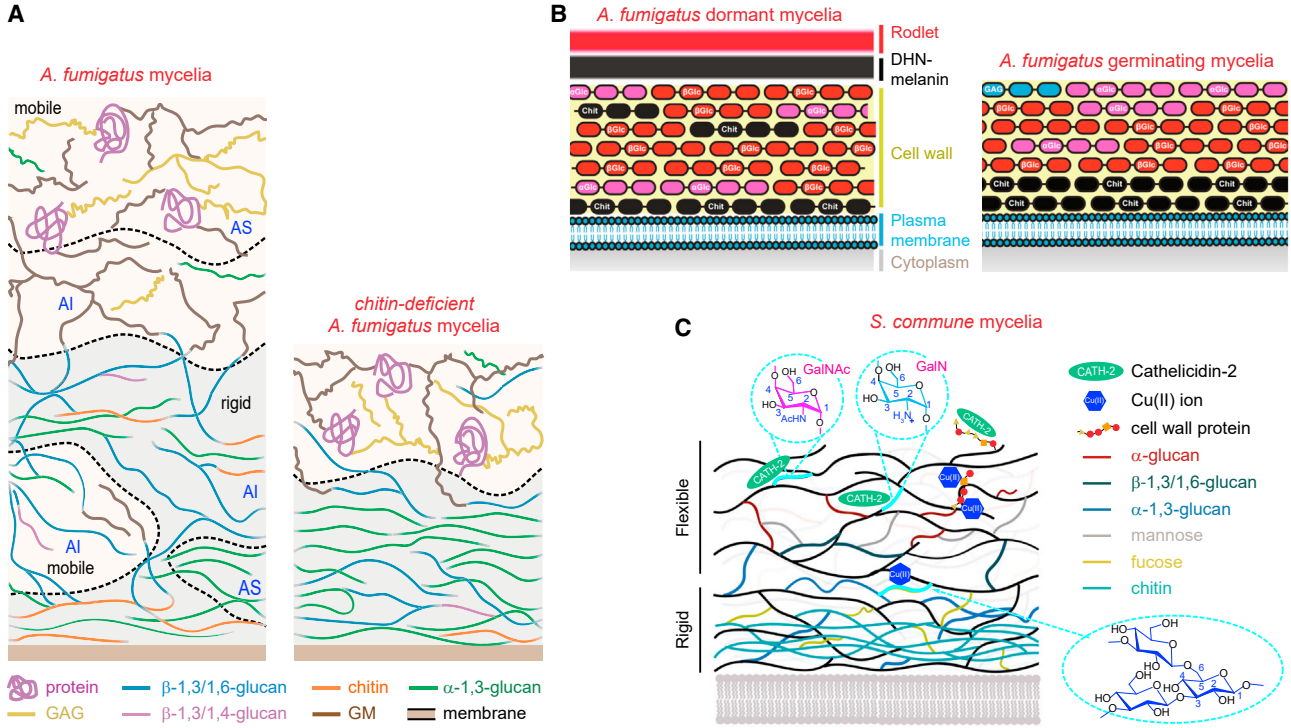

Figure 3. NMR-restrained structural models of fungal cell walls

(A) Comparative views of mycelial cell walls in the parental strain (left) and chitin-deficient mutant (right) of *A. fumigatus*.

(B) Dormant and germinating conidial cell walls of *A. fumigatus*.

(C) Mycelial cell walls of *S. commune*, highlighting the binding polysaccharides (cyan) and proteins that bind Cu(II) ions and antimicrobial peptides. Figure 3A adapted from Chakraborty et al. *Nat. Commun.* (2021), Figure 3B adapted with permission from Lamon et al. *Proc. Natl. Acad. Sci. USA* (2023), and Figure 3C adapted with permission from Safeer et al. *Eur. J. Chem.* (2022) and Ehren et al. *Cell Surf.* (2020).

known as germ tubes.[1] Following germination, the growth of hyphae initiates, leading to the formation of a colony. This mycelial colony represents an aggregated form of hyphae that invade the pulmonary tissues, causing a life-threatening disease known as aspergillosis.[90]

SsNMR analysis of the intact *Aspergillus* mycelium offers valuable insight into the structural organization of the cell wall during the vegetative growth of the fungus in the lungs. These living fungal cells exhibited high-spectral resolution, enabling the differentiation of various conformers from six major types of fungal polysaccharides, including chitin, chitosan, α-1,3-glucan, three types of β-glucan, as well as galactomannan (GM), and galactosaminogalactan (GAG) (Figure 3A).[86,91] The partially crystalline chitin has a narrow linewidth of 0.5–0.7 ppm, whereas the plant counterpart, cellulose microfibrils, shows a broader linewidth of 0.7–1.0 ppm on high-field magnets.[92] The mobile molecules present in the fungus and the plant pectin have comparable linewidths of 0.2–0.5 ppm.[93] Similar to the polymorphic structure observed in plant cellulose,[92] chitin also exhibits high polymorphism. The structural arrangement of chitin in fungi is predominantly aligned with the α-allomorph,[94] characterized by an antiparallel packing of chains.[95,96] Through ssNMR analysis, it was discovered that the rigid core of the cell wall comprises α-1,3-glucan, β-glucan, and chitin.

Of particular surprise was the identification of α-1,3-glucan's structural function, as it was previously considered insignificant in the cell wall assembly, akin to the underappreciated role of pectin in primary plant cell walls.[97] Unlike the highly mobile nature of pectin in plants, α-1,3-glucan was found to be the most rigid polysaccharide in *Aspergillus fumigatus* mycelia. It forms a tightly packed, dehydrated core through extensive physical interactions with chitin. This finding was further strengthened by the observation that α-1,3-glucans are crucial to the stiffness of the cell wall in chitin-deficient mutant (Figure 3A). Moreover, α-1,3-glucan has diverse distribution, with its physical presence in both the mobile and rigid domains and chemical existence in both the alkali-soluble and insoluble fractions, as revealed by a combined chemical and NMR approach.[91]

On the other hand, β-glucans in fungi, similar to xyloglucan in plant primary cell walls, have been proposed to play a crucial role in cross-linking. Chemical analysis has identified the presence of a small fraction of covalently linked mannan-β-1,3-glucan-chitin complex in *Aspergillus*.[87] The β-glucans encompass diverse linkages, existing as linear β-1,3-glucan, branched β-1,3/1,6-glucan, and terminal β-1,3/1,4-glucan,[90] which has not been fully characterized by ssNMR so far. However, structural analysis of β-glucans has shown that these molecules are essential for retaining water in the cell wall and contribute to the formation of a hydrated matrix. Outside of this inner domain, there is a surface shell enriched with highly mobile glycoproteins, GM and GAG.[91]

Loquet and colleagues reported the evolution of the *Aspergillus fumigatus* conidial cell wall by examining the structure of

Please cite this article in press as: Fernando et al., Polysaccharide assemblies in fungal and plant cell walls explored by solid-state NMR, Structure (2023), https://doi.org/10.1016/j.str.2023.07.012

dorC, which was the starting material, as well as swoC and gerC, which were prepared by incubating dorC by additional 5 h and 8 h, respectively.[98] Compared to dorC, the swoC exhibited isotropic growth to double its cellular size, based on which the gerC cells further underwent polarized growth, leading to the formation of germ tubes. The polysaccharides present in the rigid fractions of *A. fumigatus* conidia cell walls were found to be consistent with those of mycelial cell walls, containing chitin, α-glucan and β-glucan.[98] Another study published almost at the same time also reported highly conserved carbohydrate cores in both mycelia and conidia cell walls but using unlabeled *A. fumigatus* as enabled by the sensitivity-enhancement of MAS-DNP.[99]

In the conidial cell wall, the ratio of α-glucan to β-glucan was approximately 1:3 in dorC and gerC, but became almost equal in swoC (Figure 3B), suggesting a less stable cell wall composition required for germination.[98] Both α-glucan and β-glucan exhibited increased hydration levels in swoC and gerC compared to dorC. Interestingly, α-glucan showed high-hydration levels in all conidia cell walls,[98] whereas it was poorly hydrated in mycelia cell walls,[72] indicating differences in their structural organization. While the chitin content remained the same in the rigid portions of all three cell walls, chitin exhibited a noticeable decrease in both water-contact and structural polymorphism in gerC. This observation can be explained by a model where chitin becomes deeply embedded in the inner core and undergoes phase separation from glucans during the germinating stage (Figure 3B).[98] In addition, the presence of GAG was detected by ssNMR in both swollen and germinating conidia, but not in dormant conidia, where its biosynthesis has yet to begin. This study demonstrates the capability of cellular ssNMR to effectively uncover the structural reorganization of the fungus during the transition between morphotypes.

Triglyceride signals were also identified in the mobile phase of *A. fumigatus* cells.[98] In other fungal species, such as the melanized *C. neoformans* and *S. cerevisiae* spore cell wall, triglyceride has been identified by ssNMR as a potential building molecule of stress-resistant cell walls.[100] The biological relevance of this molecule in *A. fumigatus* and its location (e.g., as a cell wall component or an intracellular molecule) requires careful evaluation.

CELL WALL ARCHITECTURE OF *SCHIZOPHYLLUM COMMUNE*

Baldus and coworkers conducted two ssNMR investigations of *Schizophyllum commune* mycelia.[28,101] The first study involved the analysis of sequentially digested cell walls, progressively removing molecules from the cell wall.[101] The rigid domain of the cell wall is composed of chitin and β-1,3/1,6-glucan, potentially linked together, as well as α-1,3-glucan and polymeric fucose (Figure 3C). The mobile domain contains terminal hexoses included in α- and β-linked glucans. Mannose residues were also identified in the mobile phase, at least partially incorporated in mannosylated proteins. Using proton-detection methods and ultrahigh field magnets (1.2 GHz), the team further examined the binding sites of metals and antimicrobial peptides.[28] At a low-ion concentration of 0.74 mM Cu(II), the paramagnetic relaxation enhancement (PRE) effect revealed signal quenching at the primary targets, which were mainly proteins. However, at a higher ion concentration of 18.5 mM, Cu(II) ions could penetrate into the cell wall region with β-1,3/1,6-glucans. Proton-detection methods were also employed to understand the binding of many other micronutrients, such as Ca^{2+}, Mg^{2+}, and anions, to the *S. commune* cell wall.[102,103]

Additionally, the antimicrobial peptide cathelicidin-2, which inhibits *S. commune* growth, was found to primarily bind to cell wall proteins.[28] This was demonstrated through chemical shift perturbation (CSP) observed in protein backbone Cα sites and the disappearance of signals from the sidechains of charged amino acids. Interestingly, the signals of GalN/GalNAc were also affected by the peptide.[28] This observation is intriguing as cathelicidin-2 is typically positively charged with a theoretical isoelectric point (pI) in the range of 10–12 depending on the origin of the peptide.[104] At the same time, GalN can exist as cationic residues with an $-NH_3^+$ group under the pH of the fungal culture. The unidentified mechanisms underlying the association between the antimicrobial peptide and *S. commune* cell walls might inspire future studies.

INTEGRATING NMR RESTRAINTS WITH OTHER EXPERIMENTAL APPROACHES

Chemical analysis, ssNMR, diffraction methods, imaging techniques can complement each other to complete the understanding of cell wall ultrastructure. Each of these methods relies on distinct physical and chemical principles, offering unique insights into various structural aspects at different length scales. Locally, ssNMR has been combined with chemical assays and sugar analyses to confirm resonance assignment and provide detailed information on the composition and linkage patterns of carbohydrates.[105] However, the cross-linking between polymers and the extractability as probed by chemical analysis does not directly correlate with the physical packing as investigated by ssNMR.[97] For example, the majority of pectin and α-1,3-glucan are highly extractable by hot alkali, but they are both tightly associated with the crystalline core of the corresponding cell wall, cellulose in the plant and chitin in the fungus. And it has always been overlooked that a portion of pectin and α-1,3-glucan can never be fully isolated due to their physical entrapment by microfibrillar components.[55,91] Similarly, the analysis of lignin also faces challenges in establishing consistency between ssNMR and the more widely used liquid NMR.[106–108] Additionally, when it comes to polymer dynamics, it is not possible to directly combine NMR-reported parameters such as correlation time, relaxation time constants, or dipolar order parameters with values obtained from other techniques like persistence length.[65]

Diffraction methods and imaging techniques are valuable for providing structural information at nanoscale or larger length scales. Consequently, ssNMR data can complement these techniques by offering atomic-to-nanometer structural information.[109] As we discussed earlier, this strategy has been applied to rationalize the organization of spruce microfibril.[74] Moreover, a combination of MAS-DNP and cryo-electron tomography (CryoET) has been employed to examine the structure of *in vitro* synthesized cellulose fibrils, revealing that they consist of two wrapped filaments fitting into an 18-chain microfibril.[110] Cryo-electron microscopy methods have also been employed to examine the fiber arrangement in the cell wall[111–113] and the

structure of polysaccharide synthases.[114–116] Another example is the challenge of distinguishing proteins from different sources (e.g., cell walls, membrane proteins, and intracellular sources) using ssNMR alone. In such cases, confocal microscopy and atomic force microscopy (AFM) have been used to investigate the assembly of RodA rodlets in *Aspergillus*, which were found to interact with melanin on the cell surface of DorC while swoC and gerC did not support rodlet formation.[98] However, caution is necessary when attempting to bridge the findings obtained from different approaches.

CONCLUSIONS AND PERSPECTIVES

Significant progress has been made in applying ssNMR and other structural methods to unravel the complex structure of polysaccharides and associated biomacromolecules in plant and fungal cell walls. However, there are still numerous unanswered structural questions. For instance, the function of pectin in plant cell wall mechanics remains unknown, the resolution of lignin by ssNMR is insufficient, the role of GGM (galactoglucomannan) is not fully understood, and the identification of lignin-carbohydrate linkages[117] *in muro* remains challenging. Moreover, the fungal cell wall is even less explored, with many structural components, such as exopolysaccharides like glucuronoxylomannan (GXM) and galactoxylomannan (GalXM) in *Cryptococcus* capsules and β-1,6-glucan and phosphomannan in *Candida* sp., still requiring investigations. Understanding the mechanisms of cell wall remodeling in response to stress is also crucial. Recent research has unveiled that the halophilic fungus *Aspergillus sydowii* enhances the hydrophobicity and stiffness of its cell wall to resist osmotic pressure in hypersaline environments.[118] Similar changes have been observed in *A. fumigatus* during adaptation to internal stress caused by carbohydrate-deficiency and external stress such as antifungal treatment with caspofungin (unpublished results by Dickwella Widange et al.). It is essential to validate if these cell wall adaptations are universal features across various species during adaptation. Furthermore, high-resolution ssNMR techniques have been employed to address structural challenges in other organisms. An important application is the quantification and compositional analysis of carbohydrate components in algal cells, bacterial cell walls, and biofilms.[31,119–122] As ssNMR technology continues to evolve and our understanding of polysaccharide structure and cell wall assembly expands, it is now opportune to tackle important structural problems in the years to come.

ACKNOWLEDGMENTS

This work was supported by the National Institutes of Health grant AI173270. The plant cell wall research was supported by the U.S. Department of Energy, Office of Science, Basic Energy Sciences, under award number DE-SC0023702.

AUTHOR CONTRIBUTIONS

Conceptualization, T.W.; Writing—Original Draft, L.D.F. and W.Z.; Writing—Review & Editing, I.G., A.A., and T.W.

DECLARATION OF INTERESTS

The authors declare no competing interests.

REFERENCES

1. van de Veerdonk, F.L., Gresnigt, M.S., Romani, L., Netea, M.G., and Latgé, J.P. (2017). Aspergillus fumigatus morphology and dynamic host interactions. Nat. Rev. Microbiol. *15*, 661–674.
2. Gow, N.A.R., and Lenardon, M.D. (2023). Architecture of the dynamic fungal cell wall. Nat. Rev. Microbiol. *21*, 248–259. https://doi.org/10.1038/s41579-022-00796-9.
3. Cosgrove, D.J. (2022). Building an extensible cell wall. Plant Physiol. *189*, 1246–1277.
4. Cosgrove, D.J. (2005). Growth of the plant cell wall. Nat. Rev. Mol. Cell Biol. *6*, 850–861.
5. Carpita, N.C., and McCann, M.C. (2020). Redesigning plant cell walls for the biomass-based bioeconomy. J. Biol. Chem. *295*, 15144–15157.
6. Gow, N.A.R., Latge, J.P., and Munro, C.A. (2017). The fungal cell wall: structure, biosynthesis, and function. Microbiol. Spectr. *5*. FUNK-0035-2016.
7. Sarkar, P., Bosneaga, E., and Auer, M. (2009). Plant cell walls throughout evolution: towards a molecular understanding of their design principle. J. Exp. Bot. *60*, 3615–3635.
8. Paulraj, T., Wennmalm, S., Wieland, D.C.F., Riazanova, A.V., Dėdinaitė, A., Günther Pomorski, T., Cárdenas, M., and Svagan, A.J. (2020). Primary cell wall inspired micro containers as a step towards a synthetic plant cell. Nat. Commun. *11*, 958.
9. Reif, B., Ashbrook, S.E., Emsley, L., and Hong, M. (2021). Solid-State NMR Spectroscopy. Nat. Rev. Methods Primers *1*, 2.
10. Kelly, J.E., Chrissian, C., and Stark, R.E. (2020). Tailoring NMR experiments for structural characterization of amorphous biological solids: a practical guide. Solid State Nucl. Magn. Reson. *109*, 101686. https://doi.org/10.1016/j.ssnmr.2020.101686.
11. Baldus, M. (2022). Biological solid-state NMR: Integrative across different scientific disciplines. J. Struct. Biol. X *6*, 100075.
12. van der Wel, P.C.A. (2018). New applications of solid-state NMR in structural biology. Emerg. Top. Life Sci. *2*, 57–67.
13. Zhao, W., Deligey, F., Chandra Shekar, S., Mentink-Vigier, F., and Wang, T. (2022). Current limitations of solid-state NMR in carbohydrate and cell wall research. J. Magn. Reson. *341*, 107263.
14. Ghassemi, N., Poulhazan, A., Deligey, F., Mentink-Vigier, F., Marcotte, I., and Wang, T. (2022). Solid-state NMR investigations of extracellular matrixes and cell walls of algae, bacteria, fungi, and plants. Chem. Rev. *122*, 10036–10086.
15. Warnet, X.L., Arnold, A.A., Marcotte, I., and Warschawski, D.E. (2015). In-cell solid-state NMR: an emerging technique for the study of biological membranes. Biophys. J. *109*, 2461–2466. https://doi.org/10.1016/j.bpj.2015.10.041.
16. Renault, M., Tommassen-van Boxtel, R., Bos, M.P., Post, J.A., Tommassen, J., and Baldus, M. (2012). Cellular solid-state nuclear magnetic resonance spectroscopy. Proc. Natl. Acad. Sci. USA *109*, 4863–4868.
17. Gao, Y., and Mortimer, J.C. (2020). Unlocking the architecture of native plant cell walls via solid-state nuclear magnetic resonance. Methods Cell Biol. *160*, 121–143.
18. Kirui, A., Dickwella Widanage, M.C., Mentink-Vigier, F., Wang, P., Kang, X., and Wang, T. (2019). Preparation of fungal and plant materials for structural elucidation using dynamic nuclear polarization solid-state NMR. J. Vis. Exp. *144*, e59152.
19. Chatterjee, S., Prados-Rosales, R., Tan, S., Phan, V.C., Chrissian, C., Itin, B., Wang, H., Khajo, A., Magliozzo, R.S., Casadevall, A., and Stark, R.E. (2018). The melanization road more traveled by: precursor substrate effects on melanin synthesis in cell-free and fungal cell systems. J. Biol. Chem. *293*, 20157–20168. https://doi.org/10.1074/jbc.RA118.005791.
20. Laydevant, F., Mahabadi, M., Llido, P., Bourgouin, J.P., Caron, L., Arnold, A.A., Marcotte, I., and Warschawski, D.E. (2022). Growth-phase dependence of bacterial membrane lipid profile and labeling for in-cell

solid-state NMR applications. Biochim Biophys. Acta Biomembr. *1864*, 183819.

21. Shcherbakov, A.A., Medeiros-Silva, J., Tran, N., Gelenter, M.D., and Hong, M. (2022). From angstroms to nanometers: measuring interatomic distances by solid-state NMR. Chem. Rev. *122*, 9848–9879.

22. Heise, H., Seidel, K., Etzkorn, M., Becker, S., and Baldus, M. (2005). 3D NMR spectroscopy for resonance assignment and structure elucidation of proteins under MAS: novel pulse schemes and sensitivity considerations. J. Magn. Reson. *173*, 64–74.

23. Li, S., Zhang, Y., and Hong, M. (2010). 3D ^{13}C–^{13}C–^{13}C correlation NMR for de novo distance determination of solid proteins and application to a human α-defensin. J. Magn. Reson. *202*, 203–210.

24. Shekar, S.C., Zhao, W., Fernando, L.D., Hung, I., and Wang, T. (2022). A ^{13}C three-dimensional DQ-SQ-SQ correlation experiment for high-resolution analysis of complex carbohydrates using solid-state NMR. J. Magn. Reson. *336*, 107148.

25. Pauli, J., Baldus, M., van Rossum, B., de Groot, H., and Oschkinat, H. (2001). Backbone and side-chain 13C and 15N signal assignments of the α-Spectrin SH_3 domain by magic angle spinning solid-state NMR at 17.6 Tesla. Chembiochem *2*, 272–281.

26. De Paëpe, G., Lewandowski, J.R., Loquet, A., Böckmann, A., and Griffin, R.G. (2008). Proton assisted recoupling and protein structure determination. J. Chem. Phys. *129*, 245101. https://doi.org/10.1063/1.3036928.

27. Cadars, S., Lesage, A., and Emsley, L. (2005). Chemical shift correlations in disordered solids. J. Am. Chem. Soc. *127*, 4466–4476. https://doi.org/10.1021/ja043698f.

28. Safeer, A., Kleijburg, F., Bahri, S., Beriashvili, D., Veldhuizen, E.J.A., van Neer, J., Tegelaar, M., de Cock, H., Wösten, H.A.B., and Baldus, M. (2023). Probing cell-surface interactions in fungal cell walls by high-resolution 1H-detected solid-state NMR spectroscopy. Chem. Euro. J. *29*, e202202616.

29. Phyo, P., and Hong, M. (2019). Fast MAS 1H–13C correlation NMR for structural investigations of plant cell walls. J. Biomol. NMR *73*, 661–674.

30. Le Marchand, T., Schubeis, T., Bonaccorsi, M., Paluch, P., Lalli, D., Pell, A.J., Andreas, L.B., Jaudzems, K., Stanek, J., and Pintacuda, G. (2022). 1H-detected biomolecular NMR under fast magic-angle spinning. Chem. Rev. *122*, 9943–10018.

31. Bougault, C., Ayala, I., Vollmer, W., Simorre, J.P., and Schanda, P. (2019). Studying intact bacterial peptidoglycan by proton-detected NMR spectroscopy at 100 kHz MAS frequency. J. Struct. Biol. *206*, 66–72.

32. Ni, Q.Z., Daviso, E., Can, T.V., Markhasin, E., Jawla, S.K., Swager, T.M., Temkin, R.J., Herzfeld, J., and Griffin, R.G. (2013). High frequency dynamic nuclear polarization. Acc. Chem. Res. *46*, 1933–1941. https://doi.org/10.1021/ar300348n.

33. Rossini, A.J., Zagdoun, A., Lelli, M., Lesage, A., Copéret, C., and Emsley, L. (2013). Dynamic nuclear polarization surface enhanced NMR spectroscopy. Acc. Chem. Res. *46*, 1942–1951. https://doi.org/10.1021/ar300322x.

34. Takahashi, H., Ayala, I., Bardet, M., De Paëpe, G., Simorre, J.P., and Hediger, S. (2013). Solid-state NMR on bacterial cells: selective cell wall signal enhancement and resolution improvement using dynamic nuclear polarization. J. Am. Chem. Soc. *135*, 5105–5110. https://doi.org/10.1021/ja312501d.

35. Kundu, K., Mentink-Vigier, F., Feintuch, A., and Vega, S. (2019). DNP Mechanisms. Emagres *8*, 295–337. https://doi.org/10.1002/9780470034590.emrstm1550.

36. Mentink-Vigier, F., Marin-Montesinos, I., Jagtap, A.P., Halbritter, T., van Tol, J., Hediger, S., Lee, D., Sigurdsson, S.T., and De Paëpe, G. (2018). Computationally assisted design of polarizing agents for dynamic nuclear polarization enhanced NMR: the AsymPol family. J. Am. Chem. Soc. *140*, 11013–11019. https://doi.org/10.1021/jacs.8b04911.

37. Sauvée, C., Rosay, M., Casano, G., Aussenac, F., Weber, R.T., Ouari, O., and Tordo, P. (2013). Highly efficient, water-soluble polarizing agents for dynamic nuclear polarization at high frequency. Angew. Chem. *52*, 10858–10861. https://doi.org/10.1002/anie.201304657.

38. Smith, A.N., Märker, K., Hediger, S., and De Paëpe, G. (2019). Natural isotopic abundance 13C and 15N multidimensional solid-state NMR enabled by dynamic nuclear polarization. J. Phys. Chem. Lett. *10*, 4652–4662. https://doi.org/10.1021/acs.jpclett.8b03874.

39. Takahashi, H., Lee, D., Dubois, L., Bardet, M., Hediger, S., and De Paëpe, G. (2012). Rapid natural-abundance 2D 13C–13C correlation spectroscopy using dynamic nuclear polarization enhanced solid-state NMR and matrix-free sample preparation. Angew. Chem. *51*, 11766–11769. https://doi.org/10.1002/anie.201206102.

40. Zhao, W., Kirui, A., Deligey, F., Mentink-Vigier, F., Zhou, Y., Zhang, B., and Wang, T. (2021). Solid-state NMR of unlabeled plant cell walls: high-resolution structural analysis without isotopic enrichment. Biotechnol. Biofuels *14*, 14.

41. Berruyer, P., Gericke, M., Moutzouri, P., Jakobi, D., Bardet, M., Karlson, L., Schantz, S., Heinze, T., and Emsley, L. (2021). Advanced characterization of regioselectively substituted methylcellulose model compounds by DNP enhanced solid-state NMR spectroscopy. Carbohydr. Polym. *262*, 117944.

42. Kirui, A., Ling, Z., Kang, X., Widanage, M.C.D., Mentink-Vigier, F., French, A.D., and Wang, T. (2019). Atomic resolution of cotton cellulose structure enabled by dynamic nuclear polarization solid-state NMR. Cellulose *26*, 329–339.

43. Viger-Gravel, J., Lan, W., Pinon, A.C., Berruyer, P., Emsley, L., Bardet, M., and Luterbacher, J. (2019). Topology of pretreated wood fibers using dynamic nuclear polarization. J. Phys. Chem. C *123*, 30407–30415.

44. Cosgrove, D.J. (2014). Re-constructing our models of cellulose and primary cell wall assembly. Curr. Opin. Plant Biol. *22*, 122–131. https://doi.org/10.1016/j.pbi.2014.11.001.

45. Albersheim, P., Darvill, A., Roberts, K., Sederoff, R., and Staehelin, A. (2011). Plant Cell Walls, from Chemistry to Biology (Garland Science).

46. Pauly, M., Albersheim, P., Darvill, A., and York, W.S. (1999). Molecular domains of the cellulose/xyloglucan network in the cell walls of higher plants. Plant J. *20*, 629–639.

47. Atmodjo, M.A., Hao, Z., and Mohnen, D. (2013). Evolving views of pectin biosynthesis. Annu. Rev. Plant Biol. *64*, 747–779.

48. Zykwinska, A., Thibault, J.F., and Ralet, M.C. (2007). Organization of pectic arabinan and galactan side chains in association with cellulose microfibrils in primary cell walls and related models envisaged. J. Exp. Bot. *58*, 1795–1802.

49. Biswal, A.K., Atmodjo, M.A., Li, M., Baxter, H.L., Yoo, C.G., Pu, Y., Lee, Y.C., Mazarei, M., Black, I.M., Zhang, J.Y., et al. (2018). Sugar release and growth of biofuel crops are improved by downregulation of pectin biosynthesis. Nat. Biotechnol. *36*, 249–257.

50. White, P.B., Wang, T., Park, Y.B., Cosgrove, D.J., and Hong, M. (2014). Water–polysaccharide interactions in the primary cell wall of Arabidopsis thaliana from polarization transfer solid-state NMR. J. Am. Chem. Soc. *136*, 10399–10409. https://doi.org/10.1021/ja504108h.

51. Ridley, B.L., O'Neill, M.A., and Mohnen, D. (2001). Pectins: Structure, biosynthesis, and oligogalacturonide-related signaling. Phytochemistry *57*, 929–967.

52. Kirui, A., Du, J., Zhao, W., Barnes, W., Kang, X., Anderson, C.T., Xiao, C., and Wang, T. (2021). A pectin Methyltransferase modulates polysaccharide dynamics and interactions in *Arabidopsis* primary cell walls: Evidence from solid-state NMR. Carbohydr. Polym. *270*, 118370.

53. Wang, T., Zabotina, O., and Hong, M. (2012). Pectin-cellulose interactions in the *Arabidopsis* primary cell wall from two-dimensional magic-angle-spinning solid-state nuclear magnetic resonance. Biochemistry *51*, 9846–9856. https://doi.org/10.1021/Bi3015532.

54. Pérez García, M., Zhang, Y., Hayes, J., Salazar, A., Zabotina, O.A., and Hong, M. (2011). Structure and interactions of plant cell wall polysaccharides by two- and three-dimensional magic-angle-spinning solid-state NMR. Biochemistry *50*, 989–1000. https://doi.org/10.1021/Bi101795q.

55. Wang, T., Park, Y.B., Cosgrove, D.J., and Hong, M. (2015). Cellulose-pectin spatial contacts are inherent to never-dried *Arabidopsis* primary cell walls: evidence from solid-state nuclear magnetic resonance. Plant Physiol. *168*, 871–884.

56. Zhang, T., Tang, H., Vavylonis, D., and Cosgrove, D.J. (2019). Disentangling loosening from softening: insights into primary cell wall structure. Plant J. *100*, 1101–1117.

57. Zhao, W., Fernando, L.D., Kirui, A., Deligey, F., and Wang, T. (2020). Solid-state NMR of plant and fungal cell walls: a critical review. Solid State Nucl. Magn. Reson. *107*, 101660.

58. Zhang, Y., Yu, J., Wang, X., Durachko, D.M., Zhang, S., and Cosgrove, D.J. (2021). Molecular insights into the complex mechanics of plant epidermal cell walls. Science *372*, 706–711.

59. Pelloux, J., Rustérucci, C., and Mellerowicz, E.J. (2007). New insights into pectin methylesterase structure and function. Trends Plant Sci. *12*, 267–277.

60. Du, J., Anderson, C.T., and Xiao, C. (2022). Dynamics of pectic homogalacturonan in cellular morphogenesis and adhesion, wall integrity sensing and plant development. Nat. Plants *8*, 332–340.

61. Haas, K.T., Wightman, R., Meyerowitz, E.M., and Peaucelle, A. (2020). Pectin homogalacturonan nanofilament expansion drives morphogenesis in plant epidermal cells. Science *367*, 1003–1007.

62. Temple, H., Phyo, P., Yang, W., Lyczakowski, J.J., Echevarría-Poza, A., Yakunin, I., Parra-Rojas, J.P., Terrett, O.M., Saez-Aguayo, S., Dupree, R., et al. (2022). Golgi-localized putative S-adenosyl methionine transporters required for plant cell wall polysaccharide methylation. Nat. Plants *8*, 656–669.

63. Phyo, P., Gu, Y., and Hong, M. (2019). Impact of acidic pH on plant cell wall polysaccharide structure and dynamics: insights into the mechanism of acid growth in plants from solid-state NMR. Cellulose *26*, 291–304. https://doi.org/10.1007/s10570-018-2094-7.

64. Phyo, P., Wang, T., Xiao, C., Anderson, C.T., and Hong, M. (2017). Effects of pectin molecular weight changes on the structure, dynamics, and polysaccharide interactions of primary cell walls of Arabidopsis thaliana: insights from solid-state NMR. Biomacromolecules *18*, 2937–2950. https://doi.org/10.1021/acs.biomac.7b00888.

65. Phyo, P., Wang, T., Kiemle, S.N., O'Neill, H., Pingali, S.V., Hong, M., and Cosgrove, D.J. (2017). Gradients in wall mechanics and polysaccharides along growing inflorescence stems. Plant Physiol. *175*, 1593–1607. https://doi.org/10.1104/pp.17.01270.

66. Du, J., Kirui, A., Huang, S., Wang, L., Barnes, W.J., Kiemle, S.N., Zheng, Y., Rui, Y., Ruan, M., Qi, S., et al. (2020). Mutations in the pectin methyltransferase QUASIMODO2 influence cellulose biosynthesis and wall integrity in Arabidopsis. Plant Cell *32*, 3576–3597.

67. Cosgrove, D.J., and Jarvis, M.C. (2012). Comparative structure and biomechanics of plant primary and secondary cell walls. Front. Plant Sci. *3*, 204. https://doi.org/10.3389/Fpls.2012.00204.

68. Fernandes, A.N., Thomas, L.H., Altaner, C.M., Callow, P., Forsyth, V.T., Apperley, D.C., Kennedy, C.J., and Jarvis, M.C. (2011). Nanostructure of cellulose microfibrils in spruce wood. Proc. Natl. Acad. Sci. USA *108*, E1195–E1203. https://doi.org/10.1073/pnas.1108942108.

69. Dupree, R., Simmons, T.J., Mortimer, J.C., Patel, D., Iuga, D., Brown, S.P., and Dupree, P. (2015). Probing the molecular architecture of Arabidopsis thaliana secondary cell walls using two- and three-dimensional ^{13}C solid state nuclear magnetic resonance spectroscopy. Biochemistry *54*, 2335–2345. https://doi.org/10.1021/bi501552k.

70. Simmons, T.J., Mortimer, J.C., Bernardinelli, O.D., Pöppler, A.C., Brown, S.P., deAzevedo, E.R., Dupree, R., and Dupree, P. (2016). Folding of xylan onto cellulose fibrils in plant cell walls revealed by solid-state NMR. Nat. Commun. *7*, 13902. https://doi.org/10.1038/ncomms13902.

71. Grantham, N.J., Wurman-Rodrich, J., Terrett, O.M., Lyczakowski, J.J., Stott, K., Iuga, D., Simmons, T.J., Durand-Tardif, M., Brown, S.P., Dupree, R., et al. (2017). An even pattern of xylan substitution is critical for interaction with cellulose in plant cell walls. Nat. Plants *3*, 859–865. https://doi.org/10.1038/s41477-017-0030-8.

72. Kang, X., Kirui, A., Dickwella Widanage, M.C., Mentink-Vigier, F., Cosgrove, D.J., and Wang, T. (2019). Lignin-polysaccharide interactions in plant secondary cell walls revealed by solid-state NMR. Nat. Commun. *10*, 347. https://doi.org/10.1038/s41467-018-08252-0.

73. Kirui, A., Zhao, W., Deligey, F., Yang, H., Kang, X., Mentink-Vigier, F., and Wang, T. (2022). Carbohydrate-aromatic interface and molecular architecture of lignocellulose. Nat. Commun. *13*, 538.

74. Terrett, O.M., Lyczakowski, J.J., Yu, L., Iuga, D., Franks, W.T., Brown, S.P., Dupree, R., and Dupree, P. (2019). Molecular architecture of softwood revealed by solid-state NMR. Nat. Commun. *10*, 4978. https://doi.org/10.1038/s41467-019-12979-9.

75. Gao, Y., Lipton, A.S., Wittmer, Y., Murray, D.T., and Mortimer, J.C. (2020). A grass-specific cellulose-xylan interaction dominates in sorghum secondary cell walls. Nat. Commun. *11*, 6081. https://doi.org/10.1038/s41467-020-19837-z.

76. Busse-Wicher, M., Gomes, T.C.F., Tryfona, T., Nikolovski, N., Stott, K., Grantham, N.J., Bolam, D.N., Skaf, M.S., and Dupree, P. (2014). The pattern of xylan acetylation suggests xylan may interact with cellulose microfibrils as a twofold helical screw in the secondary plant cell wall of Arabidopsis thaliana. Plant J. *79*, 492–506. https://doi.org/10.1111/tpj.12575.

77. Chakraborty, A., Deligey, F., Quach, J., Mentink-Vigier, F., Wang, P., and Wang, T. (2020). Biomolecular complex viewed by dynamic nuclear polarization solid-state NMR spectroscopy. Biochem. Soc. Trans. *48*, 1089–1099.

78. Addison, B., Stengel, D., Bharadwaj, V.S., Happs, R.M., Doeppke, C., Wang, T., Bomble, Y.J., Holland, G.P., and Harman-Ware, A.E. (2020). Selective one-dimensional 13C–13C spin-diffusion solid-state nuclear magnetic resonance methods to probe spatial arrangements in biopolymers including plant cell walls, peptides, and spider silk. J. Phys. Chem. B *124*, 9870–9883.

79. Cresswell, R., Dupree, R., Brown, S.P., Pereira, C.S., Skaf, M.S., Sorieul, M., Dupree, P., and Hill, S. (2021). Importance of water in maintaining softwood secondary cell wall nanostructure. Biomacromolecules *22*, 4669–4680.

80. Li, H., Kang, X., Yang, M., Kasseney, B.D., Zhou, X., Liang, S., Zhang, X., Wen, J.L., Yu, B., Liu, N., et al. (2023). Molecular insight into the evolution of woody plant decay in the gut of termites. Sci. Adv. *9*, eadg1258.

81. Rytioja, J., Hildén, K., Yuzon, J., Hatakka, A., de Vries, R.P., and Mäkelä, M.R. (2014). Plant-polysaccharide-degrading enzymes from basidiomycetes. Microbiol. Mol. Biol. Rev. *78*, 614–649.

82. Chatterjee, S., Prados-Rosales, R., Itin, B., Casadevall, A., and Stark, R.E. (2015). Solid-state NMR reveals the carbon-based molecular architecture of Cryptococcus neoformans fungal eumelanins in the cell wall. J. Biol. Chem. *290*, 13779–13790. https://doi.org/10.1074/jbc.M114.618389.

83. Chatterjee, S., Prados-Rosales, R., Frases, S., Itin, B., Casadevall, A., and Stark, R.E. (2012). Using solid-state NMR to monitor the molecular consequences of Cryptococcus neoformans melanization with different catecholamine precursors. Biochemistry *51*, 6080–6088. https://doi.org/10.1021/bi300325m.

84. Zhong, J., Frases, S., Wang, H., Casadevall, A., and Stark, R.E. (2008). Following fungal melanin biosynthesis with solid-state NMR: Biopolyrner molecular structures and possible connections to cell-wall polysaccharides. Biochemistry *47*, 4701–4710. https://doi.org/10.1021/bi702093r.

85. Baker, R.P., Chrissian, C., Stark, R.E., and Casadevall, A. (2022). Cryptococcus neoformans melanization incorporates multiple catecholamines to produce polytypic melanin. J. Biol. Chem. *298*, 101519.

86. Kang, X., Kirui, A., Muszyński, A., Widanage, M.C.D., Chen, A., Azadi, P., Wang, P., Mentink-Vigier, F., and Wang, T. (2018). Molecular architecture of fungal cell walls revealed by solid-state NMR. Nat. Commun. *9*, 2747. https://doi.org/10.1038/S41467-018-05199-0.

87. Latgé, J.P. (2007). The cell wall: a carbohydrate armour for the fungal cell. Mol. Microbiol. *66*, 279–290. https://doi.org/10.1111/j.1365-2958.2007.05872.x.

88. Wagener, J., Striegler, K., and Wagener, N. (2020). α- and β-1,3-Glucan Synthesis and Remodeling. In The Fungal Cell Wall: An Armour and a Weapon for Human Fungal Pathogens, J.P. Latgé, ed. (Cham: Springer), pp. 53–82.

89. Wagener, J., and Loiko, V. (2017). Recent insights into the paradoxical effect of Echinocandins. J. Fungi *4*, 5.

90. Latgé, J.P., and Chamilos, G. (2019). Aspergillus fumigatus and Aspergillosis in 2019. Clin. Microbiol. Rev. *33*. e00140-00118. https://doi.org/10.1128/CMR.00140-18.

91. Chakraborty, A., Fernando, L.D., Fang, W., Dickwella Widanage, M.C., Wei, P., Jin, C., Fontaine, T., Latgé, J.P., and Wang, T. (2021). A molecular vision of fungal cell wall organization by functional genomics and solid-state NMR. Nat. Commun. *12*, 6346.

92. Wang, T., Yang, H., Kubicki, J.D., and Hong, M. (2016). Cellulose structural polymorphism in plant primary cell walls investigated by high-field 2D solid-state NMR spectroscopy and density functional theory calculations. Biomacromolecules *17*, 2210–2222. https://doi.org/10.1021/acs.biomac.6b00441.

93. Wang, T., and Hong, M. (2016). Solid-state NMR investigations of cellulose structure and interactions with matrix polysaccharides in plant primary cell walls. J. Exp. Bot. *67*, 503–514.

94. Fernando, L.D., Dickwella Widanage, M.C., Penfield, J., Lipton, A.S., Washton, N., Latgé, J.P., Wang, P., Zhang, L., and Wang, T. (2021). Structural polymorphism of chitin and chitosan in fungal cell walls from solid-state NMR and principal component analysis. Front. Mol. Biosci. *8*, 727053.

95. Heux, L., Brugnerotto, J., Desbrières, J., Versali, M.F., and Rinaudo, M. (2000). Solid state NMR for determination of degree of acetylation of chitin and chitosan. Biomacromolecules *1*, 746–751. https://doi.org/10.1021/Bm000070y.

96. Tanner, S.F., Chanzy, H., Vincendon, M., Roux, J.C., and Gaill, F. (1990). High-resolution solid-state C-13 nuclear-magnetic-resonance study of chitin. Macromolecules *23*, 3576–3583. https://doi.org/10.1021/Ma00217a008.

97. Latgé, J.P., and Wang, T. (2022). Modern biophysics redefines our understanding of fungal cell wall structure, complexity, and dynamics. mBio *13*. e01145-01122.

98. Lamon, G., Lends, A., Valsecchi, I., Wong, S.S.W., Duprès, V., Lafont, F., Tolchard, J., Schmitt, C., Mallet, A., Grélard, A., et al. (2023). Solid-state NMR molecular snapshots of Aspergillus fumigatus cell wall architecture during a conidial morphotype transition. Proc. Natl. Acad. Sci. USA *120*. e2212003120.

99. Fernando, L.D., Dickwella Widanage, M.C., Shekar, S.C., Mentink-Vigier, F., Wang, P., Wi, S., and Wang, T. (2022). Solid-state NMR analysis of unlabeled fungal cell walls from Aspergillus and Candida species. J. Struct. Biol. X *6*, 100070.

100. Chrissian, C., Lin, C.P.C., Camacho, E., Casadevall, A., Neiman, A.M., and Stark, R.E. (2020). Unconventional constituents and shared molecular architecture of the melanized cell wall of C. neoformans and spore wall of S. cerevisiae. J. Fungi *6*, 329.

101. Ehren, H.L., Appels, F.V.W., Houben, K., Renault, M.A.M., Wösten, H.A.B., and Baldus, M. (2020). Characterization of the cell wall of a mushroom forming fungus at atomic resolution using solid-state NMR spectroscopy. Cell Surf. *6*, 100046. https://doi.org/10.1016/j.tcsw.2020.100046.

102. Bahri, S., Safeer, A., Adler, A., Smedes, H., van Ingen, H., and Baldus, M. (2023). 1H-detected characterization of carbon–carbon networks in highly flexible protonated biomolecules using MAS NMR. J. Biomol. NMR *77*, 111–119.

103. Kleijburg, F.E., Safeer, A.A., Baldus, M., and Wösten, H.A. (2023). Binding of micro-nutrients to the cell wall of the fungus Schizophyllum commune. Cell Surf. *10*, 100108.

104. van Dijk, A., Molhoek, E.M., Veldhuizen, E.J.A., Bokhoven, J.L.M.T.v., Wagendorp, E., Bikker, F., and Haagsman, H.P. (2009). Identification of chicken cathelicidin-2 core elements involved in antibacterial and immunomodulatory activities. Mol. Immunol. *46*, 2465–2473.

105. Ndukwe, I.E., Black, I., Heiss, C., and Azadi, P. (2020). Evaluating the utility of permethylated polysaccharide solution NMR data for characterization of insoluble plant cell wall polysaccharides. Anal. Chem. *92*, 13221–13228.

106. Mansfield, S.D., Kim, H., Lu, F., and Ralph, J. (2012). Whole plant cell wall characterization using solution-state 2D NMR. Nat. Protoc. *7*, 1579–1589. https://doi.org/10.1038/nprot.2012.064.

107. Kim, H., and Ralph, J. (2010). Solution-state 2D NMR of ball-milled plant cell wall gels in DMSO-d6/pyridine-d5. Org. Biomol. Chem. *8*, 576–591.

108. Wang, W., Cai, J., Xu, Z., Zhang, Y., Niu, F., Gao, M., and Jun, Y. (2020). Structural characteristics of plant cell wall elucidated by solution-state 2D NMR spectroscopy with an optimized procedure. Green Process. Synth. *9*, 650–653.

109. Reichhardt, C., Joubert, L.M., Clemons, K.V., Stevens, D.A., and Cegelski, L. (2019). Integration of electron microscopy and solid-state NMR analysis for new views and compositional parameters of Aspergillus fumigatus biofilms. Med. Mycol. *57*, S239–S244.

110. Deligey, F., Frank, M.A., Cho, S.H., Kirui, A., Mentink-Vigier, F., Swulius, M.T., Nixon, B.T., and Wang, T. (2022). Structure of in vitro-synthesized cellulose fibrils viewed by cryo-electron tomography and ^{13}C natural-abundance dynamic nuclear polarization solid-state NMR. Biomacromolecules *23*, 2290–2301.

111. Nicolas, W.J., Fäßler, F., Dutka, P., Schur, F.K.M., Jensen, G., and Meyerowitz, E. (2022). Cryo-electron tomography of the onion cell wall shows bimodally oriented cellulose fibers and reticulated homogalacturonan networks. Curr. Biol. *32*, 2375–2389.e6.

112. Metskas, L.A., Wilfong, R., and Jensen, G.J. (2022). Subtomogram averaging for biophysical analysis and supramolecular context. J. Struct. Biol. X *6*, 100076.

113. Harapin, J., Eibauer, M., and Medalia, O. (2013). Structural analysis of supramolecular assemblies by cryo-electron tomography. Structure *21*, 1522–1530.

114. Jiménez-Ortigosa, C., Jiang, J., Chen, M., Kuang, X., Healey, K.R., Castellano, P., Boparai, N., Ludtke, S.J., Perlin, D.S., and Dai, W. (2021). Preliminary structural elucidation of β-(1,3)-glucan synthase from Candida glabrata using cryo-electron tomography. J. Fungi *7*, 120.

115. Hu, X., Yang, P., Chai, C., Liu, J., Sun, H., Wu, Y., Zhang, M., Zhang, M., Liu, X., and Yu, H. (2023). Preliminary structural elucidation of β-(1,3)-glucan synthase from Candida glabrata using cryo-electron tomography. Nature *616*, 190–198.

116. Purushotham, P., Ho, R., and Zimmer, J. (2020). Architecture of a catalytically active homotrimeric plant cellulose synthase complex. Science *369*, 1089–1094.

117. Giummarella, N., Pu, Y., Ragauskas, A.J., and Lawoko, M. (2019). A critical review on the analysis of lignin carbohydrate bonds. Green Chem. *21*, 1573–1595.

118. Fernando, L.D., Perez-Llano, Y., Dickwella Widanage, M.C., Martinez-Avila, L., Lipton, A.S., Gunde-Cimerman, N., Latge, J.P., Bastista-Garcia, R.A., and Wang, T. (2023). Structural organization of the cell wall of halophilic fungi. Preprint at bioRxiv. https://doi.org/10.1101/2023.04.15.537024.

119. Romaniuk, J.A.H., and Cegelski, L. (2015). Bacterial cell wall composition and the influence of antibiotics by cell-wall and whole-cell NMR. Philos. Trans. R. Soc. B *370*, 20150024. https://doi.org/10.1098/rstb.2015.0024.

120. Reichhardt, C., Lim, J.Y., Rice, D., Fong, J.N., and Cegelski, L. (2014). Structure and function of bacterial biofilms by solid-state NMR. Biophys. J. *106*, 192a. https://doi.org/10.1016/j.bpj.2013.11.1139.

121. Poulhazan, A., Dickwella Widanage, M.C., Muszyński, A., Arnold, A.A., Warschawski, D.E., Azadi, P., Marcotte, I., and Wang, T. (2021). Identification and quantification of glycans in whole cells: architecture of microalgal polysaccharides described by solid-state nuclear magnetic resonance. J. Am. Chem. Soc. *143*, 19374–19388.

122. Arnold, A.A., Bourgouin, J.P., Genard, B., Warschawski, D.E., Tremblay, R., and Marcotte, I. (2018). Whole cell solid-state NMR study of *Chlamydomonas reinhardtii* microalgae. J. Biomol. NMR *70*, 123–131. https://doi.org/10.1007/s10858-018-0164-7.